

## Fatty acid synthase inhibition with Orlistat promotes apoptosis and reduces cell growth and lymph node metastasis in a mouse melanoma model

Marco A. Carvalho<sup>1</sup>, Karina G. Zecchin<sup>2</sup>, Fabiana Seguin<sup>1</sup>, Débora C. Bastos<sup>1</sup>, Michelle Agostini<sup>1</sup>, Ana Lúcia C.A. Rangel<sup>1</sup>, Sílvia S. Veiga<sup>3</sup>, Helena F. Raposo<sup>4</sup>, Helena C.F. Oliveira<sup>4</sup>, Massimo Loda<sup>5</sup>, Ricardo D. Coletta<sup>1</sup> and Edgard Graner<sup>1\*</sup>

<sup>1</sup>Department of Oral Diagnosis, School of Dentistry of Piracicaba, State University of Campinas (UNICAMP), Piracicaba, Sao Paulo, Brazil

<sup>2</sup>Department of Clinical Pathology, School of Medical Sciences, State University of Campinas (UNICAMP), Campinas, Sao Paulo, Brazil

<sup>3</sup>Department of Cell Biology, Federal University of Paraná, Brazil

<sup>4</sup>Department of Physiology and Biophysics, Institute of Biology, State University of Campinas (UNICAMP), Campinas, Sao Paulo, Brazil

<sup>5</sup>Medical Oncology, Dana-Farber Cancer Institute and Pathology Department, Brigham and Women's Hospital, Harvard Medical School, Boston, MA

Fatty acid synthase (FASN) is the enzyme responsible for the endogenous synthesis of the saturated fatty acid palmitate. In contrast to most normal cells, malignant cells depend on FASN activity for growth and survival. In fact, FASN is overexpressed in a variety of human cancers including cutaneous melanoma, in which its levels of expression are associated with a poor prognosis and depth of invasion. Here, we show that the specific inhibition of FASN activity by the antiobesity drug Orlistat or siRNA is able to significantly reduce proliferation and promote apoptosis in the mouse metastatic melanoma cell line B16-F10. These results prompted us to verify the effect of FASN inhibition on the metastatic process in a model of spontaneous melanoma metastasis, in which B16-F10 cells injected in the peritoneal cavity of C57BL/6 mice metastasize to the mediastinal lymph nodes. We observed that mice treated with Orlistat 48 hr after the inoculation of B16-F10 cells exhibited a 52% reduction in the number of mediastinal lymph node metastases, in comparison with the control animals. These results suggest that FASN activity is essential for B16-F10 melanoma cell proliferation and survival while its inactivation by Orlistat significantly reduces their metastatic spread. The chemical inhibition of FASN activity could have a potential benefit in association with the current chemotherapy for melanoma.

© 2008 Wiley-Liss, Inc.

**Key words:** melanoma; fatty acid synthase; metastasis; Orlistat; B16-F10 cells

Endogenous fatty acid synthesis from the small carbon precursors acetyl-CoA and malonyl-CoA is dependent on the activity of fatty acid synthase (FASN, EC2.3.1.85). In most of the cells, FASN is downregulated by the dietary fatty acids, with exception of lipogenic tissues as liver, lactating breast, fetal lung and adipose tissue.<sup>1,2</sup> Recent studies provide compelling evidence that neoplastic lipogenesis is essential for cancer cell survival. In fact, several human epithelial malignancies, such as those of prostate, breast, ovary, bladder, lung, stomach and oral cavity, melanoma as well as soft tissue sarcomas overexpress FASN.<sup>3–16</sup> For some of these tumors, such as prostate, breast and ovarian cancers and melanoma,<sup>4,5,9,12</sup> FASN overexpression has also been associated with a poor prognosis. Experimental studies have shown that FASN inhibition reduces cell proliferation by blocking DNA replication during S-phase, induces apoptosis,<sup>17–20</sup> and decrease the size of prostate, ovarian and breast cancer xenografts.<sup>3,21,22</sup> In addition, the inhibition of FASN activity has a chemopreventive effect in the breast cancer transgenic neu-N mouse model.<sup>23</sup> Orlistat (tetrahydrolipstatin) is an irreversible inhibitor of pancreatic and gastric lipases clinically used because of its antiobesity properties that also blocks the activity of the thioesterase domain of FASN.<sup>24</sup> In fact, FASN inhibition by Orlistat reduces proliferation and promotes apoptosis in prostate, breast and stomach cancer cell lines<sup>24–27</sup> and has shown antitumor activity by inhibiting the growth of prostate cancer xenografts.<sup>24</sup>

The regulation of FASN abundance in cancer cells is complex and occurs at the transcriptional or posttranslational levels. Progesterone stimulates FASN expression in breast cancer cell lines<sup>28</sup> whereas androgens or epidermal-growth factor (EGF) upregulate FASN expression and activity in the androgen-dependent prostate cancer cell line LNCaP.<sup>29–32</sup> On the other hand, the FASN protein can be degraded by the ubiquitin-proteasome system, in a process that is controlled by its interaction with the deubiquitinating enzyme USP2a.<sup>33</sup>

Malignant melanoma is a chemotherapy-resistant aggressive tumor that arises in the skin and less frequently affects oral and anogenital mucosa, esophagus, meninges and the eyes. The incidence of this type of skin cancer has increased during the last 50 years in the United States<sup>34</sup> and the high mortality rates are directly associated with its intrinsic ability to metastatically spread to other organs. Immunohistochemical detection of the FASN protein has been recently associated with Breslow thickness, suggesting a poor prognosis for patients affected by cutaneous melanoma.<sup>12,35</sup> In this work, we present evidence that FASN activity is necessary for the proliferation of the highly metastatic murine melanoma B16-F10 cells. In addition, we show that FASN specific inhibition with the antiobesity drug Orlistat promotes apoptosis and reduces B16-F10 spontaneous metastasis from the peritoneal cavity to the mediastinal lymph nodes of C57BL/6 mice.

### Material and methods

#### Cell culture

B16-F10 murine melanoma cells were maintained in RPMI medium (Invitrogen, Carlsbad, CA) supplemented with 2 or 10% fetal bovine serum (FBS, Cultilab, Campinas, SP, Brazil) and antibiotic/antimycotic solution (Invitrogen) at 37°C in a humidified atmosphere with 5% CO<sub>2</sub>. The nontumorigenic murine melanocyte lineage Melan-A (a gift of Dr. Miriam G. Jasiulionis, UNIFESP, São Paulo, Brazil) was cultured in RPMI with 5% FBS.<sup>36</sup> LNCaP, PC-3 and SK-MEL cells were grown in RPMI 10% FBS, MCF7 and A2058 cells were grown in DMEM (Invitrogen)

Grant sponsor: Fundação de Amparo à Pesquisa do Estado de São Paulo (FAPESP); Grant number: 04/13903-0, 02/08030-1. Grant sponsor: FAPESP fellowships; Grant number: 05/52631-8, 05/50297-3, 04/13904-6, 04/06397-0. Grant sponsor: Conselho Nacional de Desenvolvimento Científico e Tecnológico fellowships; Grant number: PIBIC-CNPq, 151125/2005-8.

\*Correspondence to: Department of Oral Diagnosis, School of Dentistry of Piracicaba, State University of Campinas (UNICAMP), Avenida Limeira 901, CP 52, Arêão, Piracicaba, Sao Paulo, 13414-018, Brazil. Fax: 55-19-2106-5218. E-mail: egraner@fop.unicamp.br

Received 9 November 2007; Accepted after revision 20 June 2008

DOI 10.1002/ijc.23835

Published online 3 September 2008 in Wiley InterScience (www.interscience.wiley.com).

containing 10% FBS. To block FASN activity, cerulenin (Sigma-Aldrich, St. Louis, MO) or Orlistat (Xenical<sup>®</sup>, Roche, Switzerland) were added to the culture medium at the concentrations described in the figure legends. For the proliferation curves, cells were seeded in 24-well plates ( $5 \times 10^3$ /well) in RPMI containing 2 or 10% FBS and after 24-hr incubated in serum-free medium for the same period of time. After that, RPMI containing FBS plus FASN inhibitors or their respective controls (dimethylsulfoxide—DMSO—or absolute ethanol) was added and cells from triplicate wells were trypsinized and counted in an automated cell counter (Coulter Counter Z1, Beckman, CA).

#### Preparation of Orlistat solutions

For cell culture experiments, Orlistat was extracted from Xenical capsules according to Knowles *et al.*<sup>27</sup> Each pill was solubilized in 1 ml of ethanol, insoluble products removed by centrifugation (12,000g for 5 min) and the supernatant (250 mM of Orlistat) stored at  $-80^\circ\text{C}$ . Mice were treated with Orlistat solutions prepared according to Kridel *et al.*<sup>24</sup> with some modifications. Briefly, the content of each capsule (120 mg) of Orlistat was solubilized in 33% ethanol during  $\sim 30$  min and vortexed every 10 min. After centrifugation for 5 min at 12,000g, supernatants were retrieved and stored at  $-80^\circ\text{C}$ .

#### Indirect immunofluorescence

B16-F10 cells ( $2 \times 10^4$ /well) were plated in 8-well chamber slides (Lab Tek, Nunc, Naperville, IL) and grown for  $\sim 24$  hr. After fixation in 3.7% paraformaldehyde, cells were washed twice with phosphate-buffered saline (PBS) and incubated for 1 hr at room temperature with anti-FASN primary antibodies (Transduction Laboratories, Lexington, KY) diluted at 1:250 in PBS containing 0.1% bovine serum albumin (BSA, Sigma). Cells were washed with PBS, incubated with FITC-conjugated anti-mouse IgG (1:500, Vector Laboratories, Burlingame, CA) for 1 hr, washed again and mounted in Vectashield with DAPI (Vector Laboratories). Documentations were made in a Leica DMR microscope equipped with epifluorescence (Leica Microsystems, Germany).

#### MTT assay

Cell viability was determined using 3-(4,5-dimethylthiazol-2-yl)-2,5-diphenyltetrazolium bromide (MTT, Sigma). Briefly, MCF7, LNCaP, PC-3 and B16-F10 cells were plated in each well of 6-well culture plates ( $2 \times 10^4$  cells). After 24 hr, the cell culture medium was replaced by fresh medium containing different concentrations of Orlistat and incubated for more 48 hr. Cells were then washed in PBS, trypsinized and incubated with 2.5 mg/mL of MTT in PBS at  $37^\circ\text{C}$  for 1.5 hr. After that, 10% SDS in 0.01 M HCl was added to dissolve the cell pellets and following an incubation of 15 min centrifuged at 3,000 rpm for 5 min. Supernatants were transferred to 96-well plates and the absorbance determined with a microplate reader (Bio-Rad, Hercules, CA, USA) at 540 nm. Cell viability was expressed as the percentage of viable cells relative to the controls. The experiment was repeated 3 times independently.

#### RNA interference (RNAi)-mediated silencing of FASN expression

The 25-mer RNA molecules were chemically synthesized, annealed and purified by the manufacturer (Stealth RNAi, Invitrogen). Three sequences targeting *Mus musculus* FASN (NM\_00798) were used, corresponding to nucleotides 940-964 (5' CAA TGA TGG CCA ACC GGC TCT CTT T 3'), 3408-3432 (5' TGG GAA GAC CCG AAC TCC AAG TTA T 3') and 5841-5865 (5' CCT CTG GGC ATG GCT ATC TTC TTG A 3'). B16-F10 cells grown to 50% confluence were transfected with 200 nM of a mixture containing equal parts of the 3 FASN siRNAs using a liposome method according to manufacturer's instructions (Lipofectamine 2000, 3  $\mu\text{l}/\text{ml}$ , Invitrogen). As negative controls, cells were transfected with equimolar concentrations of a nonspecific control oligo (Stealth RNAi Negative Control Duplexes, Medium GC

Duplex, Invitrogen). Transfections were performed in 60- or 100-mm dishes and 24-, 48- or 72-hr posttransfection cells were collected for assessing FASN knockdown, cell cycle and apoptosis.

#### Flow cytometry

Samples were analyzed in a FACSCalibur flow cytometer (BD Biosciences, San Jose, CA) equipped with an argon laser and CellQuest software (version 4.1). Ten thousand events were collected for each sample. B16-F10 cell populations were identified by their light-scattering characteristics, enclosed in electronic gates and analyzed for the intensity of the fluorescent probe signal. Cells were harvested ( $10^6$  cells/ml), washed with PBS and resuspended in a binding buffer containing annexin V-FITC (1:500). Apoptosis was quantified by FACS analysis as the number of annexin V-FITC positive cells. For cell cycle analysis, B16-F10 cells were seeded in 100-mm dishes and after 24-hr serum starved for the same period of time. After this period, cell culture medium supplemented with 2% of FBS plus Orlistat or ethanol was added and kept for different periods of time. Cells were fixed in cold 70% ethanol, stored at  $-20^\circ\text{C}$ , washed in cold PBS and treated with 10  $\mu\text{g}/\text{ml}$  of RNase during 1 hr at  $37^\circ\text{C}$ . After staining with 50  $\mu\text{g}/\text{ml}$  of propidium iodide during 2 hr at  $4^\circ\text{C}$ , the distribution of cells in the cell cycle was analyzed by flow cytometry. Caspase-3 activation was measured as recommended by the manufacturer (Calbiochem, San Diego, CA). Briefly, B16-F10 cells ( $10^6$  cells/ml) were incubated with FITC-DEVD-FMK (1:300) in serum free medium for 40 min at  $37^\circ\text{C}$ , washed, resuspended in culture medium and analyzed by flow cytometry.

#### Total protein and melanin extractions

For protein lysate preparation B16-F10 cells were scraped and lysed in a buffer containing 10% sucrose, 1% NP-40, 20 mM Tris-HCl (pH 8.0), 137 mM NaCl, 10% glycerol, 2 mM EDTA, 10 mM NaF, 1 mM  $\text{Na}_3\text{VO}_4$ , 1 mM phenylmethylsulfonyl fluoride (PMSF), 10  $\mu\text{g}/\text{ml}$  soybean trypsin inhibitor, 1  $\mu\text{g}/\text{ml}$  leupeptin and 1  $\mu\text{g}/\text{ml}$  aprotinin. Protein lysates were placed on ice for 30 min, vortexed every 10 min and cleared by centrifugation at 12,000g for 15 min at  $4^\circ\text{C}$ . The supernatants were retrieved and frozen at  $-80^\circ\text{C}$  until use. The protein concentrations were determined using the Bradford method.<sup>37</sup> Melanin extractions were performed according to Ando *et al.*<sup>38</sup> Briefly, cell pellets ( $\sim 10^6$  cells) were centrifuged at 1,000g for 5 min and washed twice with PBS. The number of remaining cells after treatment with 500  $\mu\text{M}$  of Orlistat was counted and used to normalize the cell pellets exposed to 100 or 250  $\mu\text{M}$  of the drug and the controls. After further centrifugation, supernatants were discarded and precipitated cells resuspended in 200  $\mu\text{l}$  of distilled water, followed by the addition of 1 ml of ethanol-ether 1:1 (vol/vol). After 15 min, the mixture was centrifuged as described earlier and the precipitate solubilized in 1 ml of 1 M NaOH/10% DMSO at  $80^\circ\text{C}$  for 30 min. The absorbance of the melanin solutions was measured at 470 nm in a spectrophotometer (Spectronic Genesys 2, Rochester, NY).

#### Western blotting

Forty micrograms of each protein lysate were resolved on SDS-polyacrylamide gels, transferred onto nitrocellulose membranes (Protran, Schleicher & Schuell, Keene, NH) and stained with Ponceau S (Sigma) to verify the transfer efficiency and equal sample loading. The membranes were blocked with 5% nonfat dry milk in Tris-HCl pH 7.6 containing 150 mM NaCl and 0.1% Tween-20 (TBST) and probed for 2 hr at room temperature with antibodies against FASN (1:3,000—Transduction Laboratories), p27<sup>Kip1</sup> (1:1,000—Transduction Laboratories), Skp2 (1:1,000—Santa Cruz Biotechnology, Santa Cruz, CA), or anti-beta actin (AC-15) (1:40,000—Sigma). Membranes were washed in TBST and then incubated with horseradish peroxidase (HRP)-conjugated secondary antibodies diluted at 1:1,000, washed again and the reactions developed with an enhanced chemiluminescence detection system (ECL detection kit, Amersham Pharmacia Biotech, Arlington

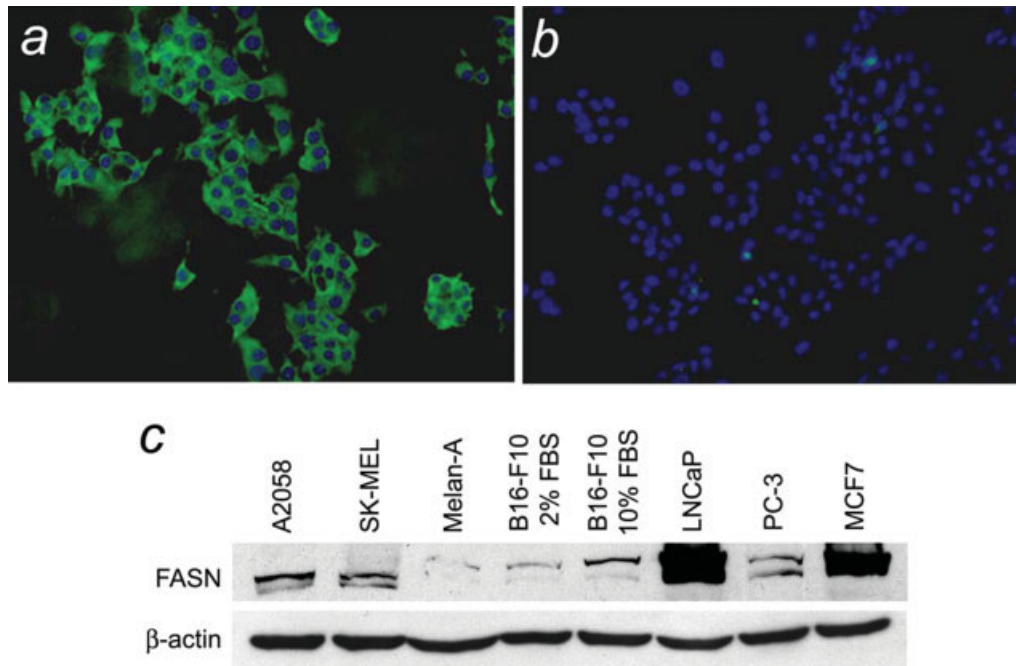


**FIGURE 1** – FASN production by B16-F10 mouse melanoma cells. (a) Immunofluorescence reaction for the FASN protein showing an intense and homogeneously distributed intracytoplasmic positivity in B16-F10 melanoma cells. (b) Negative control (nuclei were stained in blue with DAPI; original magnification:  $\times 200$ ). (c) Western blotting reaction comparing FASN production in B16-F10 cells with other cell lines. The FASN band in B16-F10 cells grown in 10% FBS was stronger than in the presence of 2% FBS and less intense than in A2058 or SK-MEL human melanoma cells. Melan-A cells showed a weak FASN protein band and LNCaP cells were the higher producers, followed by MCF7 cells. FASN production in PC-3 cells was similar to the human melanoma cell lines.

Heights, IL) according to manufacturer's instructions. Membranes were exposed to high performance chemiluminescence films (Hyperfilm<sup>TM</sup> ECL, Amersham Biosciences, Little Chalfont, Buckinghamshire, UK).

#### Melanoma model for spontaneous metastasis

B16-F10 mouse melanoma cells are capable to promote both experimental or spontaneous metastasis in C57BL/6 mice.<sup>39</sup> Cells were grown until 60–70% confluence in RPMI 10% FBS, trypsinized, resuspended in PBS and injected ( $25 \times 10^4$  cells) in the peritoneal cavity of C57BL/6 mice with 8–9 weeks of age. Forty-eight hours after cell inoculations, the animals started to be treated with daily IP injections of Orlistat (240 mg/kg) or the equivalent amount of vehicle (60  $\mu$ l of 33% ethanol). After 12–15 days from the cell injections, mice were sacrificed by cervical dislocation, carefully dissected and the metastatic mediastinal lymph nodes counted. Samples of the primary tumors were collected and immediately frozen in liquid nitrogen. The lungs, liver, thymus, brain, as well as the primary tumors and metastatic lymph nodes of each animal were embedded in paraffin, cut (3  $\mu$ m) and mounted on silane-coated glass slides for hematoxylin and eosin (H&E) staining. The intensities of the melanin pigmentation in the metastatic mediastinal lymph nodes were classified as negative, weak or strong in a blinded analysis performed by 2 of the authors (MAC and EG) and the area of each metastatic lymph node calculated with the Scion Image software (Scion Corporation, USA). This experiment was made 3 times independently with the approval of the Committee for Ethics in Animal Research of the State University of Campinas—UNICAMP.

#### Total lipid biosynthesis

Total lipid synthesis was measured *in vivo* and in cultured B16-F10 cells. Each animal was injected intraperitoneally with 20 mCi of [<sup>3</sup>H] water (GE Healthcare, UK) dissolved in isotonic saline solution as described previously.<sup>40–42</sup> One-hour later, blood samples were obtained from the retro-orbital plexus of anesthetized

mice and the intraperitoneal primary tumors were excised, minced, saponified and hexane extracted. Radioactivity in the total lipid extract (lipogenesis) was measured in a LS6000 Beckman Beta Counter. The specific activity of [<sup>3</sup>H] water was measured in plasma in triplicates. The rates of lipid synthesis were calculated as nanomoles of [<sup>3</sup>H] water incorporated into lipids per gram of tissue in 1 hr (nmol/g/h). B16-F10 cells ( $10^7$ ) were resuspended in 1 ml of RPMI containing 2% FBS, 1 mCi of [<sup>3</sup>H] water and Orlistat (250 or 500  $\mu$ M) or ethanol as control. The flasks were gassed with O<sub>2</sub>/CO<sub>2</sub>, sealed with stoppers and incubated for 60 min at 37°C in a shaking water bath. Lipid extractions<sup>43</sup> were performed by the addition of methanol–chloroform 2:1 (3.75 ml) and agitation during 30 min at room temperature. The mixtures were centrifuged at 10,000g for 15 min, the supernatants saved and the protein pellets were resuspended in 1 ml of PBS. The procedure was repeated and combined extracts were diluted in 5 ml of a chloroform–water mixture (1:1), acidified to pH 3.0–4.0 with HCl and centrifuged as described earlier. The chloroform layer was removed and saved, and the aqueous layer again extracted with the same volume of chloroform. The combined chloroform extracts were evaporated and the lipogenesis determined in 1 ml of scintillation solution.

#### Results

##### *FASN activity is necessary for the proliferation and survival of B16-F10 cells*

As depicted in Figures 1a and 1b, FASN protein was easily detected by indirect immunofluorescence in regularly growing B16-F10 melanoma cells, which were characterized by a finely granular positivity uniformly distributed throughout the cytoplasm. FASN protein production in B16-F10 cells and other cell lines was analyzed by western blotting (Fig. 1c). The FASN band was stronger in total protein extracts obtained from B16-F10 cells cultured in 10% than in 2% FBS and less intense than the observed in human melanoma cell lines A2058 and SK-MEL. Interestingly,

the nontumorigenic murine melanocyte cells (Melan-A) showed less FASN protein than B16-F10 cells and, as expected, LNCaP prostate cancer cells showed the highest FASN production (Fig. 1c). To verify whether the inhibition of FASN activity can modify the growth rate of these cells, the natural FASN inhibitor

cerulenin or Orlistat were added to the culture medium. Because Orlistat did not affect B16-F10 cell growth in standard culture conditions (cell culture medium supplemented with 10% FBS), we next performed MTT experiments in order to compare the B16-F10 cell viability with other cancer cell lines, in the presence of Orlistat. As depicted in Figure 2a, Orlistat did not reduce the viability of B16-F10 cells in the presence of 10% FBS as it can be clearly observed in prostate (LNCaP and PC-3) and breast (MCF7) cancer cells. On the other hand, the viability of B16-F10 cells was decreased by 250 and 500  $\mu\text{M}$  of the drug when cultured with 2% FBS (Fig. 2a). The growth curve shown in Figure 2b shows an important inhibitory effect of Orlistat at 250  $\mu\text{M}$  in comparison with the vehicle control ( $p < 0.001$ , Mann-Whitney test). Thereafter, all the experiments were performed in low serum concentration. On the other hand, 5  $\mu\text{g/ml}$  of cerulenin significantly reduced cell proliferation in comparison with the respective DMSO control even in the presence of 10% FBS (Fig. 2c;  $p < 0.001$ , Mann-Whitney test). The results from the proliferation curves were further confirmed by the experiments shown in Figures 3g–3i, in which we analyzed the melanin content and lipid biosynthesis in B16-F10 treated with Orlistat. To better characterize the antiproliferative properties of Orlistat on B16-F10 mouse melanoma cells, we next performed flow cytometry experiments, which showed a gradual increase over time (from 0 to 48 hr) of the G0-G1 population as well as a clear decline of the S phase, in comparison with untreated cells. Figure 2d illustrates the percentage of cells in each phase of the cell cycle after 36 hr of incubation in cell culture medium containing 250 or 500  $\mu\text{M}$  of Orlistat. A similar effect was observed when B16-F10 cells were treated with siRNA specific for FASN (but not with the control siRNA) (Figs. 2e and 2f). Indeed, western blotting analysis of protein lysates obtained from cells treated with Orlistat showed accumulation of p27<sup>Kip1</sup>, a negative regulator of the G1/S transition and a downregulation of Skp2, which is essential for the proteasomal degradation of p27<sup>Kip1</sup> (Fig. 2g). Interestingly, the intensity of FASN protein bands were reduced in Orlistat-treated B16-F10 cells (Fig. 2g). The endogenous synthesis of fatty acids is also important for B16-F10 cell survival, because cells grown in the presence of 250 or 500  $\mu\text{M}$  of Orlistat for 20 hr had an increase of 34.56 and

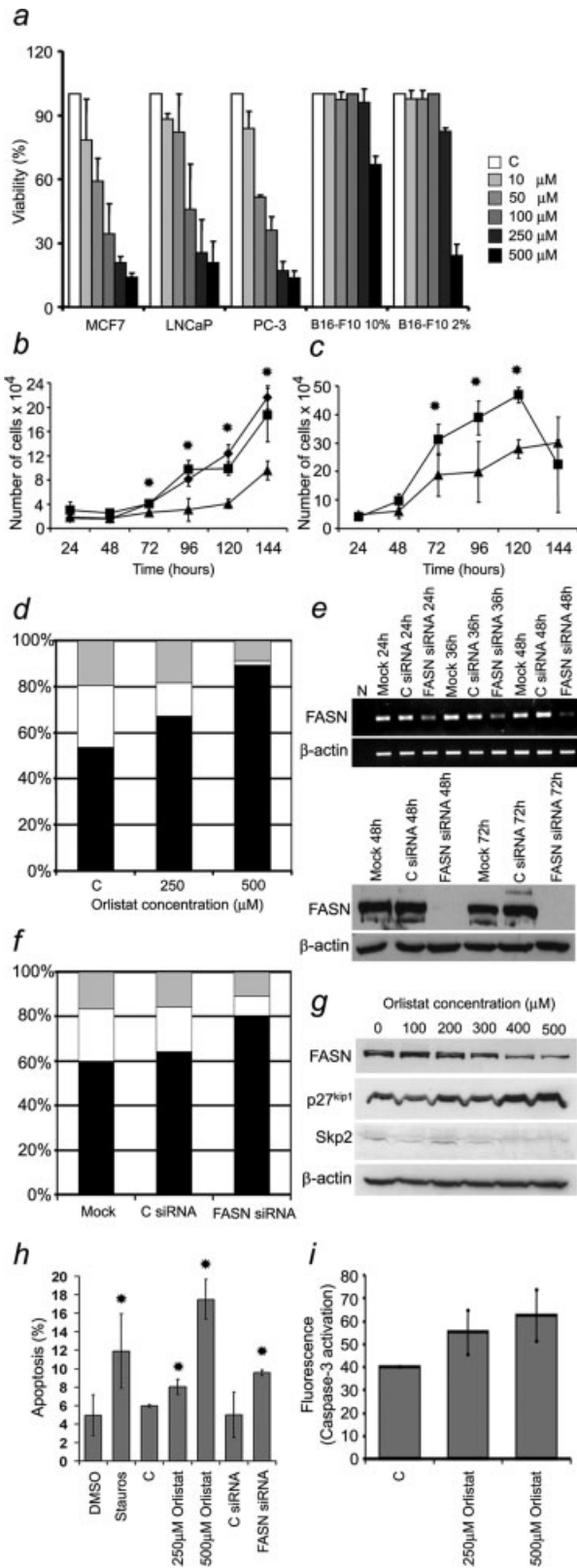


**FIGURE 2** – FASN activity is necessary for B16-F10 cell growth and survival. (a) MTT experiments showed that the viability of B16-F10 cells in the presence of 10% FBS was not affected by Orlistat at 10, 50, 100 and 250  $\mu\text{M}$  and reduced at 500  $\mu\text{M}$  of the drug. Prostate (LNCaP and PC-3) and breast (MCF7) cancer cell lines were strongly affected by low concentrations of Orlistat. B16-F10 cell viability was decreased at 250  $\mu\text{M}$  and severely reduced at 500  $\mu\text{M}$  of Orlistat in medium containing low serum. (b) Orlistat at 250  $\mu\text{M}$  ( $\blacktriangle$ ) significantly inhibited the growth of B16-F10 cells in medium supplemented with 2% of FBS in comparison with the ethanol control ( $\blacklozenge$ ). At 100  $\mu\text{M}$ , Orlistat did not affect B16-F10 cell proliferation ( $\blacksquare$ ) ( $*p < 0.001$ , Mann-Whitney test). (c) The inhibition of FASN activity with 5  $\mu\text{g/ml}$  of cerulenin strongly reduced the proliferation of B16-F10 cells cultured in standard conditions (10% of FBS) ( $\blacktriangle$ ) in comparison with the respective DMSO controls ( $\blacksquare$ ). (d) Cell cycle analysis by flow cytometry showed that the incubation of B16-F10 cells with Orlistat for 36 hr enhances the G0-G1 population and dramatically reduces the number of cells in the S phase ( $\blacksquare$  = G0/G1,  $\square$  = S,  $\blacksquare$  = G2/M). (e) Semiquantitative RT-PCR and western-blotting reactions showing that siRNA for FASN reduced the amount of FASN mRNA mainly after 48 hr and efficiently knocked-down the FASN protein after 48 and 72 hr. (f) siRNA specific for FASN (but not the control siRNA) had the same effect as Orlistat in B16-F10 cells by promoting cell cycle arrest. (g) Western blotting analysis of protein extracts prepared from Orlistat-treated B16-F10 cells revealed accumulation of p27<sup>Kip1</sup> and downregulation of Skp2 and FASN proteins. (h) Annexin V experiment showing that the treatment of B16-F10 cells with Orlistat for 20 hr (especially at 500  $\mu\text{M}$ ) as well as siRNA for FASN induce apoptotic cell death ( $*p < 0.05$ , *t*-test, DMSO: DMSO control, Staurosporin, C: ethanolic control, C siRNA: control siRNA). (i) Orlistat-induced apoptosis in B16-F10 cells was associated with caspase-3 activation.

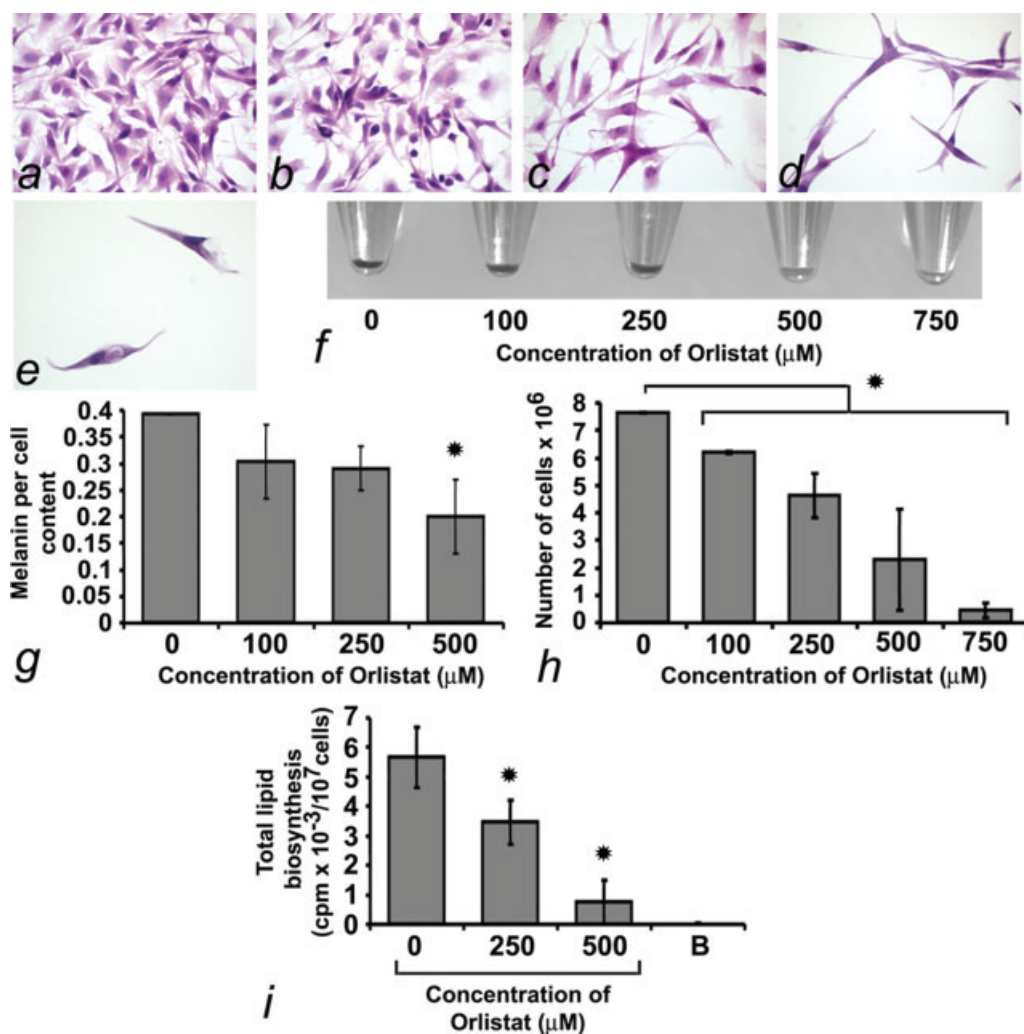


**FIGURE 3** – FASN inhibition by Orlistat reduced the melanin content, cell growth and total lipid biosynthesis by B16-F10 cells. (a–e) Melanoma cells exposed to 100 (b) and 250 (c)  $\mu\text{M}$  of Orlistat showed scarce cytoplasm and long cell projections in comparison with the control cells (a). In the presence of 500 (d) and 750 (e)  $\mu\text{M}$  of the drug cells became fusiform (H&E staining; original magnification:  $\times 200$ ). (f) Cells were cultured in the presence of 100–750  $\mu\text{M}$  of Orlistat during 48 hr and harvested by trypsinization. Cell pellets were almost completely discolored at 500 and 750  $\mu\text{M}$  of Orlistat (the cell pellets from control, 100, 250 and 500  $\mu\text{M}$  were normalized and contain  $10^6$  cells while the pellets obtained from the 750  $\mu\text{M}$  condition were smaller due to the cytotoxic effect of the drug). (g) Melanin was extracted from the cell pellets represented in (f), except from the 750  $\mu\text{M}$  condition, and the OD of the supernatants graphically expressed as the amount of melanin per cell content. (h) The total number of cells was determined by automatic cell counting before the melanin extractions shown in (g). Note that 100 and 250  $\mu\text{M}$  of Orlistat inhibited B16-F10 cell growth whereas 500 and 750  $\mu\text{M}$  were cytotoxic since the number of cells counted after Orlistat treatment was lower than the number of cells in the beginning of the experiment ( $3.5 \times 10^5$  cells). (i) Inhibition of FASN activity by Orlistat in B16-F10 cells was analyzed by incorporation of [ $^3\text{H}$ ] water and revealed a significant reduction of the total lipid biosynthesis ( $p < 0.05$ ,  $t$ -test, B: blank). [Color figure can be viewed in the online issue, which is available at [www.interscience.wiley.com](http://www.interscience.wiley.com).]

193.62%, respectively, of apoptotic cell death over the control values (Fig. 2h), which was associated with caspase-3 activation (Fig. 2i). Apoptosis was also significantly enhanced when the FASN protein was knocked-down by the transfection with siRNA against FASN (Fig. 2h).

To verify the effectiveness of Orlistat in order to block FASN activity in B16-F10 cells, we first used Oil Red O staining. In contrast with the LNCaP cells used as positive controls,<sup>44</sup> in which lipid droplets were clearly stained, we were not able to observe lipid accumulation in the cytoplasm of B16-F10 cells. Considering that the saturated fatty acid palmitate (C16:0, the end-product of FASN) is able to protect tyrosinase from proteasomal degradation and thus regulate the melanin content of B16-F10 cells,<sup>38,45</sup> we next performed melanin extractions from cells grown in the presence of different concentrations of Orlistat. Indeed, as shown in Figures 3f and 3g control B16-F10 cell pellets (treated with etha-

nol only) had a dark gray or black color whereas the cell pellets obtained from Orlistat-treated cultures contained less melanin, being almost completely discolored at 500 and 750  $\mu\text{M}$ . These results suggest that FASN activity is specifically inhibited by Orlistat in a dose-dependent manner leading to the reduction of the melanin synthesis, phenomenon that can be attributed to the previously demonstrated effect of palmitate on tyrosinase half-life in B16-F10 cells.<sup>38,45</sup> At the end of the incubations with Orlistat, cells were counted and, as expected, a strong reduction of the cell growth was observed at 250 and 500  $\mu\text{M}$ , whereas 750  $\mu\text{M}$  of the drug caused cell death (Fig. 3h). FASN activity inhibition by Orlistat was further confirmed by incorporation studies of [ $^3\text{H}$ ] water, which showed a significant reduction of the total lipid production (Fig. 3i). In addition to its effects on melanin synthesis and cell growth, FASN inhibition promoted morphological changes in B16-F10 cells, which were evidenced by the scarce cytoplasm and

longer cell projections of the Orlistat-treated cells in comparison with control cells (Figs. 3a–3e). At the highest concentration of the drug, B16-F10 cells became predominantly fusiform (Figs. 3d and 3e). The biological mechanisms underlying these phenotypic changes are unknown; however, fusiform B16-F10 cells were also observed after the treatment with siRNA for FASN (data not shown).

#### *FASN inhibition reduces spontaneous lymph node metastasis from the peritoneal cavity*

Approximately 14 days after intraperitoneal (IP) inoculation of B16-F10 cells all mice showed abdominal enlargement, which was variable in size and shape. Despite the well characterized anti-obesity properties of Orlistat, there were no significant weight differences between the control and treated groups (data not shown). This fact may be associated with the route of administration (IP), because when Orlistat is orally used its effects are confined into the gastrointestinal tract.<sup>46</sup> Another possible explanation could be the short period of treatment, since in this experimental model the animals die 12–15 days after B16-F10 cell inoculation due to the aggressive tumor growth in the peritoneal cavity. However, it is worth mentioning here that mice from the Orlistat-treated group showed slower locomotor activity than the control animals few days before the sacrifice, probably due to unknown systemic side effects of the drug. The abdominal primary tumors of the control mice consisted of a soft mass generally found at the side of the cell injections (Fig. 4a). In contrast, primary tumors from Orlistat-treated mice were in small groups distributed throughout the peritoneal cavity (Fig. 4b, Table I). Histological examination confirmed that these islands of tumor tissue were not invading the abdominal organs. One animal from the treated group did not develop primary tumor (Table I). Macroscopic examination of the thoracic cavity allowed the quantification of mediastinal lymph nodes with melanoma metastases (Fig. 4c, 4e–4g), histologically confirmed (Figs. 5d and 5e). After 3 independent experiments, Orlistat-treated mice had 52% less metastatic mediastinal lymph nodes than the control animals, with 75 and 39 metastatic lymph nodes found in the control and Orlistat-treated group, respectively (average of 3.57 per animal in the control group and 1.95 per animal in the Orlistat-treated group;  $p < 0.001$ , *t*-test) (Figs. 4f and 4g, Table I). One animal of the control group had macroscopic metastatic foci in its left lung (Fig. 4d), microscopically confirmed (data not shown). To check if the IP injections of Orlistat were systemically effective in the studied animals, incorporation of [<sup>3</sup>H] water in the total lipids and Oil Red O staining in frozen sections were performed. As depicted in Figure 5c, the total lipid biosynthesis was significantly inhibited in the primary tumor tissues of Orlistat-treated mice. In addition, the hepatocytes of control mice were rich in lipid droplets, in contrast with the weakly stained sections of Orlistat-treated mice (Figs. 5a and 5b). Indeed, small vacuoli probably corresponding to the lipid-containing vesicles in the hepatocytes of the control animals were also observed in paraffin sections stained with H&E (data not shown). These results suggest that Orlistat was effective to reduce FASN activity. Microscopically, melanin accumulation in the tumor cells infiltrating the mediastinal lymph nodes of the control mice was more evident than in lymph nodes from Orlistat-treated animals (Figs. 5d and 5e), observation that further substantiate the effectiveness of FASN inhibition. In addition, primary tumor tissues of control and Orlistat-treated mice were similar, with intense melanin pigmentation, numerous blood vessels and areas of necrosis (Figs. 5f and 5g).

#### Discussion

In the present study, we assessed the role of *de novo* fatty acid synthesis in melanoma cell growth and metastatic capacity in an animal model. We demonstrated that FASN is expressed by murine melanoma B16-F10 cells and is essential for their proliferation and survival, since FASN inhibition significantly reduced the cell growth and promoted apoptosis. Importantly, this work sug-

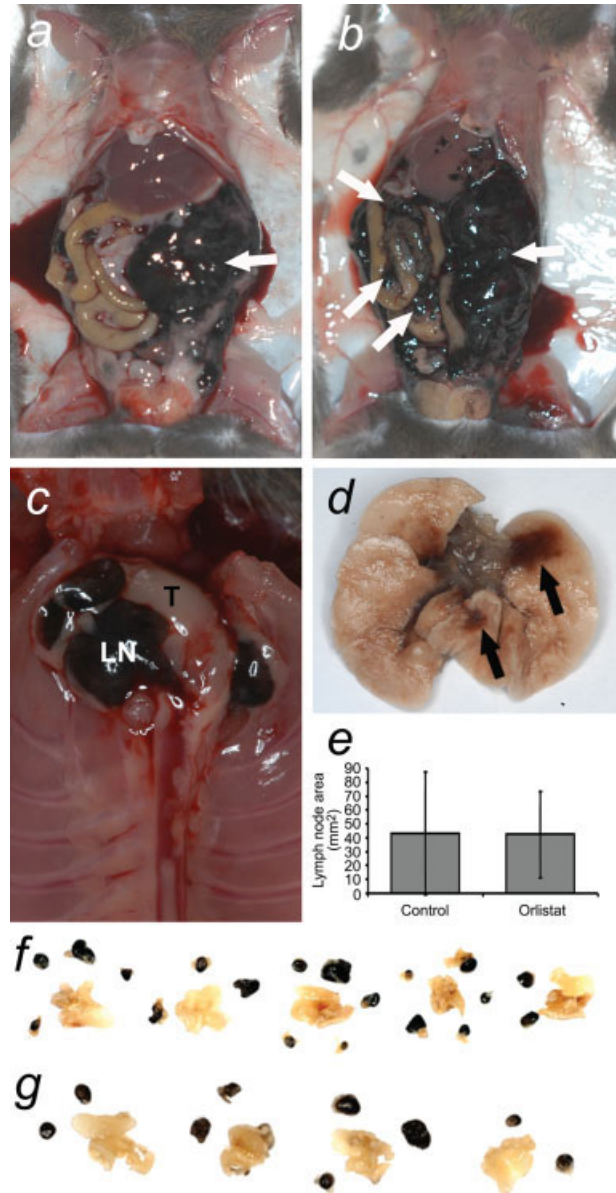


**FIGURE 4** – Primary tumors of control mice were generally found at the side of cell injections and consisted of a soft and relatively circumscribed mass (a). (b) Primary tumors observed in Orlistat-treated group had many small groups of noninvasive tumor cells spread into the peritoneal cavity. (c) Metastatic mediastinal lymph nodes (LN) were easily identified due to their black color next to the thymus (T). (d) Gross appearance of the melanoma metastasis found in the left lung of one mouse of the control group. (e) Mean area of lymph nodes removed from control and Orlistat-treated animals ( $p = 0.66$ , Mann-Whitney test). (f and g) Representative experiment showing the dissected lymph nodes and thymus; control mice (f) had more than twice ( $n = 19$ ) metastatic lymph nodes than Orlistat-treated group (g) ( $n = 9$ ). [Color figure can be viewed in the online issue, which is available at [www.interscience.wiley.com](http://www.interscience.wiley.com).]

gests that FASN activity has a role in the spontaneous metastatic spread of B16-F10 cells from the peritoneal cavity of C57BL/6 mice through the lymphatic circulation. The antiproliferative and proapoptotic effects of FASN inhibition were also recently described in A-375 human melanoma cells.<sup>47</sup>

Clinicopathological and experimental data indicate that FASN is a potential chemotherapeutic or chemopreventive target for several human malignancies. FASN is essential during embryogenesis,

**TABLE 1** – DEGREE OF MEDIASTINAL LYMPH NODE INVOLVEMENT, PRESENCE OF DISTANT METASTASIS AND PRIMARY TUMOR FRAGMENTATION AFTER TREATMENT WITH 240 mg/kg OF ORLISTAT

	Experiment	Number of mice	Metastatic LN (average)	Distant metastasis	Primary tumor fragmentation (%)
Control	1	6	16 (2.66)	1	0 (0)
	2	5	18 (3.6)	0	0 (0)
	3	10	41 (4.1)	0	0 (0)
Total		21	75 (3.57)*	1 <sup>1</sup>	0 (0)
Orlistat	1	6	7 (1.16)	0	6 (100)
	2	4	9 (2.25)	0	3 <sup>2</sup> (75)
	3	9	23 (2.55)	0	9 (100)
Total		19	39 (2.05)*	0	18 (94.7)

One animal of the Orlistat-treated group (first experiment) did not develop detectable primary tumor.

LN, Lymph node.

<sup>1</sup>To the lungs. <sup>2</sup>One primary tumor in this group was very small.

\* $p < 0.001$ ,  $t$ -test.

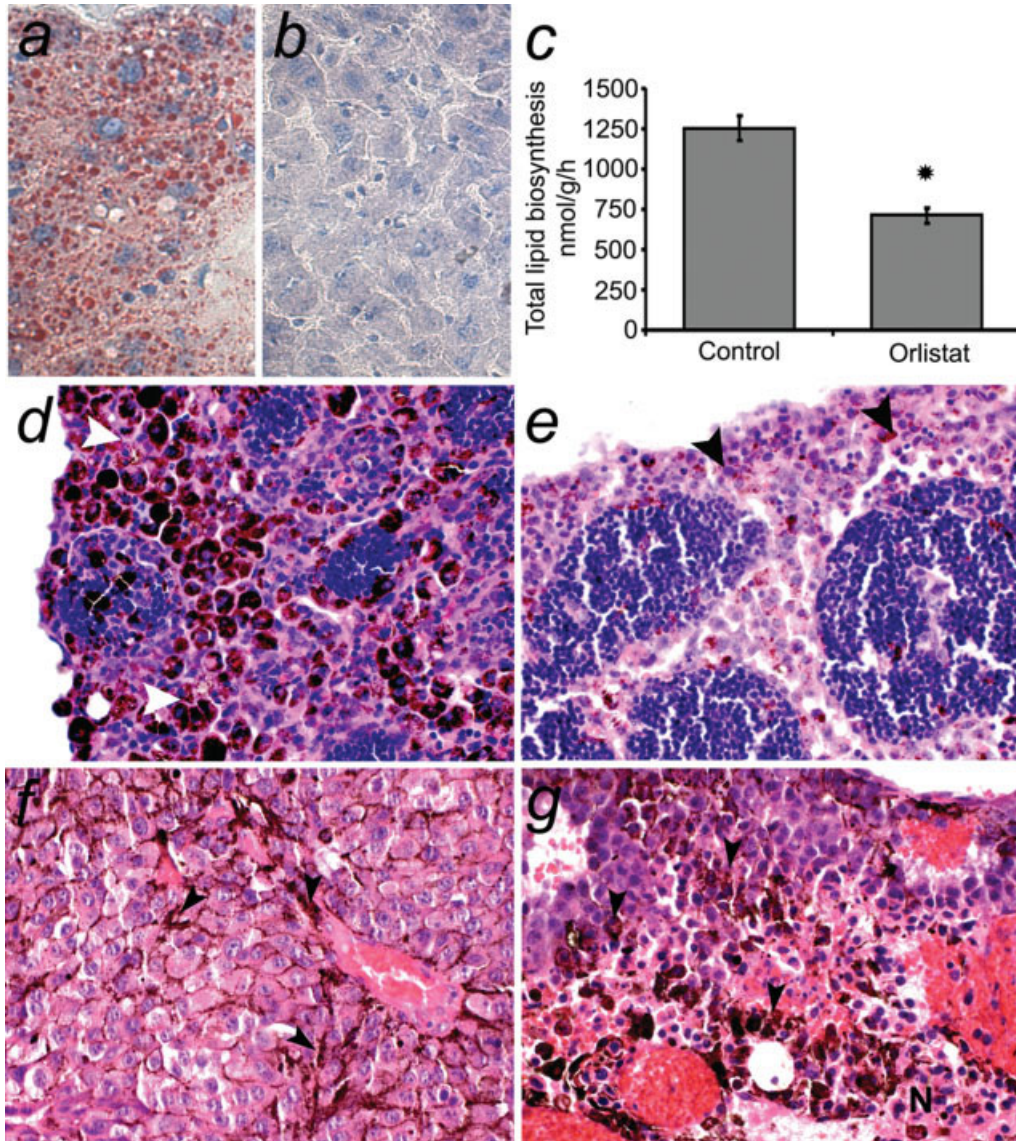


**FIGURE 5** – Microscopic findings of the liver, lymph node metastasis, and primary tumors and effect of Orlistat in the tumor tissues. (a) Representative Oil Red O staining in a frozen section from the liver of a control animal, showing a large number of lipid droplets in the cytoplasm of the hepatocytes, in contrast with the almost completely negative section from an Orlistat-treated mouse (b). (c) The primary tumors of Orlistat-treated mice showed a significant reduction in the total lipid biosynthesis, as revealed by the incorporation of [ $^3$ H] water ( $p < 0.001$ ,  $t$ -test). (d) Representative metastatic lymph node from a control animal infiltrated in its periphery by heavily pigmented melanoma cells (arrowheads). (e) Representative metastatic lymph node removed from an Orlistat-treated mouse showing comparatively low melanin accumulation (arrowheads). Control (f) and Orlistat-treated primary tumors (g) were histologically similar and characterized by anaplastic melanoma cells rich in melanin (arrowheads), calibrous blood vessels and areas of necrosis (N). (a, b, d–g: original magnification  $\times 400$ ).

since Fasn<sup>-/-</sup> and Fasn<sup>+/-</sup> mice die *in utero* even in the presence of a diet rich in saturated fatty acids.<sup>48</sup> Its expression is upregulated in a variety of human cancers and seems to be a prognostic marker for some of these tumors.<sup>3-15,49</sup> The intensity of FASN immunohistochemical positivity is stronger in human malignant melanoma than in conventional nevi or Spitz nevi,<sup>55</sup> being associated with the Breslow thickness<sup>12,35</sup> and suggested as a molecular prognostic marker.<sup>12</sup> Moreover, FASN was among 128 differentially expressed genes in a cDNA microarray study of adenocarcinoma metastatic tissues.<sup>50</sup> Although the exact role of FASN in malignant cells is not elucidated, it is clear that FASN specific inhibitors block cell cycle progression and cause apoptosis in many cancer cell lines<sup>17-19</sup> and are capable of decreasing the size of prostate and ovarian cancer xenografts.<sup>3,21,24</sup> Moreover, FASN has a role in the synthesis of phospholipids partitioning into detergent-resistant microdomains in LNCaP cells, which are implicated in signal transduction, intracellular trafficking and cell polarization and migration.<sup>51</sup>

The site of tumor cell implantation may affect in many ways the distribution and number of metastases. In this work, we chose to ectopically inject the highly metastatic B16-F10 melanoma cells<sup>52,53</sup> in the peritoneal cavity of C57BL/6 mice based on our previous observation that in this way mediastinal metastatic lymph nodes are detected in almost all cases (Veiga SS, unpublished results). Therefore, this seems to be a good model for the study of new antimetastatic drugs. IP inoculation of the B16 melanoma-derived BL6 cell line in C57BL/6 mice has been previously shown to promote metastasis in the lungs, spleen and thymus<sup>34</sup> while B16-F10 cells have been used to produce metastasis after subcutaneous or intravenous implantation in mice.<sup>55-57</sup> In this study, the size of the primary tumors was not evaluated because of their diffuse mode of growth inside the peritoneal cavity. Interestingly, in contrast with the relatively well circumscribed primary tumors observed in the control animals, Orlistat-treated tumors were more dispersed among the abdominal organs. The biological mechanisms by which FASN inhibition with Orlistat caused these macroscopic differences still need to be elucidated. Primary tumors from both studied groups were histologically similar and characterized by the presence of many mitotic cells, intense melanin accumulation, extensive areas of necrosis and neoangiogenesis.

Here, we demonstrate that FASN inhibition by Orlistat significantly reduces metastasis to mediastinal lymph nodes, which were easily localized because of their enhanced size and black color. The exact role of FASN activity in the metastatic process is still unknown. It is possible to speculate that Orlistat reduced metastasis in this study as a consequence of the cell growth inhibition or enhanced apoptosis in the primary tumor. Additionally, the drug may reduce cell viability in the lymphatic or blood circulation, interfere with their growth and colonization in the lymph node sinus, or inhibit neovasculogenesis. In fact, recent results demonstrate that Orlistat has antiangiogenic properties by preventing the display of VEGFR2 at the endothelial cell surface, which in turn inhibit their proliferation and neovascularization in a *ex vivo* assay.<sup>58</sup> As used in the present study the blood levels of Orlistat may reach 16  $\mu\text{M}$ ,<sup>24</sup> in contrast with the higher effective concentrations observed in our cell culture experiments (250–500  $\mu\text{M}$ ). Indeed, B16-F10 cells were more resistant to FASN interference by Orlistat than prostate or breast cancer cell lines.<sup>24,27</sup> The abdominal lymphatic drainage of the daily Orlistat intraperitoneal injections may provide high concentrations of the drug in the mediastinal lymph nodes and hence reduce metastatization. Histological examination of the metastatic mediastinal lymph nodes revealed more melanin accumulation in the tumor cells of control animals than in the Orlistat-treated ones, which may indicate effective FASN inhibition.

Taken together, the results here presented suggest that FASN is a potential chemotherapeutic target for melanoma. Further studies using orthotopic melanoma cell implantation will be necessary to the better understanding of the role of the endogenous neoplastic lipogenesis in melanoma cell progression and metastasis. Additionally, there is a need for the characterization of the systemic and possible side effects of this new route of Orlistat administration.

#### Acknowledgements

MAC, FS, ALCAR, MA, DCB and KGZ were supported by FAPESP fellowships. DCB and KGZ were supported by Conselho Nacional de Desenvolvimento Científico e Tecnológico fellowships. We thank Dr. Maria Luiza C.S. De Oliveira and Claudinei Ferreira for the Assistance with the Olredo Staining.

#### References

- Kuhajda FP. Fatty-acid synthase and human cancer: new perspectives on its role in tumor biology. *Nutrition* 2000;16:202–8.
- Weiss L, Hoffmann GE, Schreiber R, Andres H, Fuchs E, Korber E, Kolb HJ. Fatty-acid biosynthesis in man, a pathway of minor importance. Purification, optimal assay conditions, and organ distribution of fatty-acid synthase. *Biol Chem Hoppe Seyler* 1986;367:905–12.
- Pizer ES, Wood FD, Heine HS, Romantsev FE, Pasternack GR, Kuhajda FP. Inhibition of fatty acid synthesis delays disease progression in a xenograft model of ovarian cancer. *Cancer Res* 1996;56:1189–93.
- Gansler TS, Hardman W, III, Hunt DA, Schaffel S, Hennigar RA. Increased expression of fatty acid synthase (OA-519) in ovarian neoplasms predicts shorter survival. *Hum Pathol* 1997;28:686–92.
- Alo PL, Visca P, Marci A, Mangoni A, Botti C, Di Tondo U. Expression of fatty acid synthase (FAS) as a predictor of recurrence in stage I breast carcinoma patients. *Cancer* 1996;77:474–82.
- Krontiras H, Roye GD, Beenken SE, Myers RB, Mayo MS, Peters GE, Grizzle WE. Fatty acid synthase expression is increased in neoplastic lesions of the oral tongue. *Head Neck* 1999;21:325–9.
- Piyathilake CJ, Frost AR, Manne U, Bell WC, Weiss H, Heimbürger DC, Grizzle WE. The expression of fatty acid synthase (FASE) is an early event in the development and progression of squamous cell carcinoma of the lung. *Hum Pathol* 2000;31:1068–73.
- Dhanasekaran SM, Barrette TR, Ghosh D, Shah R, Varambally S, Kurachi K, Pienta KJ, Rubin MA, Chinnaiyan AM. Delineation of prognostic biomarkers in prostate cancer. *Nature* 2001;412:822–6.
- Shurbaji MS, Kalbfleisch JH, Thurmond TS. Immunohistochemical detection of a fatty acid synthase (OA-519) as a predictor of progression of prostate cancer. *Hum Pathol* 1996;27:917–21.
- Kusakabe T, Nashimoto A, Honma K, Suzuki T. Fatty acid synthase is highly expressed in carcinoma, adenoma and in regenerative epithelium and intestinal metaplasia of the stomach. *Histopathology* 2002;40:71–9.
- Swinnen JV, Roskams T, Joniau S, Van Poppel H, Oyen R, Baert L, Heyns W, Verhoeven G. Overexpression of fatty acid synthase is an early and common event in the development of prostate cancer. *Int J Cancer* 2002;98:19–22.
- Innocenzi D, Alo PL, Balzani A, Sebastiani V, Silipo V, La Torre G, Ricciardi G, Bosman C, Calvieri S. Fatty acid synthase expression in melanoma. *J Cutan Pathol* 2003;30:23–8.
- Rossi S, Graner E, Febbo P, Weinstein L, Bhattacharya N, Onody T, Bubleky G, Balk S, Loda M. Fatty acid synthase expression defines distinct molecular signatures in prostate cancer. *Mol Cancer Res* 2003;1:707–15.
- Visca P, Sebastiani V, Pizer ES, Botti C, De Carli P, Filippi S, Monaco S, Alo PL. Immunohistochemical expression and prognostic significance of FAS and GLUT1 in bladder carcinoma. *Anticancer Res* 2003;23:335–9.
- Takahiro T, Shinichi K, Toshimitsu S. Expression of fatty acid synthase as a prognostic indicator in soft tissue sarcomas. *Clin Cancer Res* 2003;9:2204–12.
- Rossi S, Ou W, Tang D, Bhattacharya N, Dei Tos AP, Fletcher JA, Loda M. Gastrointestinal stromal tumours overexpress fatty acid synthase. *J Pathol* 2006;209:369–75.
- Furuya Y, Akimoto S, Yasuda K, Ito H. Apoptosis of androgen-independent prostate cell line induced by inhibition of fatty acid synthesis. *Anticancer Res* 1997;17:4589–93.
- Pizer ES, Chrest FJ, DiGiuseppe JA, Han WF. Pharmacological inhibitors of mammalian fatty acid synthase suppress DNA replication and induce apoptosis in tumor cell lines. *Cancer Res* 1998;58:4611–15.
- Li JN, Gorospe M, Chrest FJ, Kumaravel TS, Evans MK, Han WF, Pizer ES. Pharmacological inhibition of fatty acid synthase activity

- produces both cytostatic and cytotoxic effects modulated by p53. *Cancer Res* 2001;61:1493–9.
20. Zhou W, Simpson PJ, McFadden JM, Townsend CA, Medghalchi SM, Vadlamudi A, Pinn ML, Ronnett GV, Kuhajda FP. Fatty acid synthase inhibition triggers apoptosis during S phase in human cancer cells. *Cancer Res* 2003;63:7330–7.
  21. Pizer ES, Pflug BR, Bova GS, Han WF, Udan MS, Nelson JB. Increased fatty acid synthase as a therapeutic target in androgen-independent prostate cancer progression. *Prostate* 2001;47:102–10.
  22. Pizer ES, Thupari J, Han WF, Pinn ML, Chrest FJ, Frehywot GL, Townsend CA, Kuhajda FP. Malonyl-coenzyme-A is a potential mediator of cytotoxicity induced by fatty-acid synthase inhibition in human breast cancer cells and xenografts. *Cancer Res* 2000;60:213–18.
  23. Alli PM, Pinn ML, Jaffee EM, McFadden JM, Kuhajda FP. Fatty acid synthase inhibitors are chemopreventive for mammary cancer in neu-N transgenic mice. *Oncogene* 2005;24:39–46.
  24. Kridel SJ, Axelrod F, Rozenkrantz N, Smith JW. Orlistat is a novel inhibitor of fatty acid synthase with antitumor activity. *Cancer Res* 2004;64:2070–5.
  25. Menendez JA, Vellon L, Lupu R. Orlistat: from antiobesity drug to anticancer agent in Her-2/neu (erbB-2)-overexpressing gastrointestinal tumors? *Exp Biol Med (Maywood)* 2005;230:151–4.
  26. Menendez JA, Vellon L, Lupu R. Antitumoral actions of the anti-obesity drug orlistat (Xenical™) in breast cancer cells: blockade of cell cycle progression, promotion of apoptotic cell death and PEA3-mediated transcriptional repression of Her2/neu (erbB-2) oncogene. *Ann Oncol* 2005;16:1253–67.
  27. Knowles LM, Axelrod F, Browne CD, Smith JW. A fatty acid synthase blockade induces tumor cell-cycle arrest by down-regulating Skp2. *J Biol Chem* 2004;279:30540–5.
  28. Lacasa D, Le Liepvre X, Ferre P, Dugail I. Progesterone stimulates adipocyte determination and differentiation 1/sterol regulatory element-binding protein 1c gene expression. potential mechanism for the lipogenic effect of progesterone in adipose tissue. *J Biol Chem* 2001;276:11512–16.
  29. Swinnen JV, Esquet M, Goossens K, Heyns W, Verhoeven G. Androgens stimulate fatty acid synthase in the human prostate cancer cell line LNCaP. *Cancer Res* 1997;57:1086–90.
  30. Swinnen JV, Heemers H, Deboel L, Fougelle F, Heyns W, Verhoeven G. Stimulation of tumor-associated fatty acid synthase expression by growth factor activation of the sterol regulatory element-binding protein pathway. *Oncogene* 2000;19:5173–81.
  31. Heemers H, Maes B, Fougelle F, Heyns W, Verhoeven G, Swinnen JV. Androgens stimulate lipogenic gene expression in prostate cancer cells by activation of the sterol regulatory element-binding protein cleavage activating protein/sterol regulatory element-binding protein pathway. *Mol Endocrinol* 2001;15:1817–28.
  32. Van de Sande T, De Schrijver E, Heyns W, Verhoeven G, Swinnen JV. Role of the phosphatidylinositol 3'-kinase/PTE/Akt kinase pathway in the overexpression of fatty acid synthase in LNCaP prostate cancer cells. *Cancer Res* 2002;62:642–6.
  33. Graner E, Tang D, Rossi S, Baron A, Migita T, Weinstein LJ, Lechpammer M, Huesken D, Zimmermann J, Signoretti S, Loda M. The isopeptidase USP2a regulates the stability of fatty acid synthase in prostate cancer. *Cancer Cell* 2004;5:253–61.
  34. Ries LAG, Eisner MP, Kosary CL, Hankey BF, Miller BA, Clegg L, Mariotto A, Fay MP, Feuer EJ, Edwards BK. SEER Cancer statistics review, 1975–2000. Bethesda, MD: National Cancer Institute, 2003.
  35. Kapur P, Rakheja D, Roy LC, Hoang MP. Fatty acid synthase expression in cutaneous melanocytic neoplasms. *Mod Pathol* 2005;18:1107–12.
  36. Bennett DC, Cooper PJ, Hart IR. A line of non-tumorigenic mouse melanocytes, syngeneic with the B16 melanoma and requiring a tumour promoter for growth. *Int J Cancer* 1987;39:414–18.
  37. Bradford MM. A rapid and sensitive method for the quantitation of microgram quantities of protein utilizing the principle of protein-dye binding. *Anal Biochem* 1976;72:248–54.
  38. Ando H, Funasaka Y, Oka M, Ohashi A, Furumura M, Matsunaga J, Matsunaga N, Hearing VJ, Ichihashi M. Possible involvement of proteolytic degradation of tyrosinase in the regulatory effect of fatty acids on melanogenesis. *J Lipid Res* 1999;40:1312–16.
  39. Khanna C, Hunter K. Modeling metastasis in vivo. *Carcinogenesis* 2005;26:513–23.
  40. Dietschy JM, Spady DK. Measurement of rates of cholesterol synthesis using tritiated water. *J Lipid Res* 1984;25:1469–76.
  41. Osono Y, Woollett LA, Herz J, Dietschy JM. Role of the low density lipoprotein receptor in the flux of cholesterol through the plasma and across the tissues of the mouse. *J Clin Invest* 1995;95:1124–32.
  42. Oliveira HC, Cosso RG, Alberici LC, Maciel EN, Salerno AG, Dorigheo GG, Velho JA, de Faria EC, Vercesi AE. Oxidative stress in atherosclerosis-prone mouse is due to low antioxidant capacity of mitochondria. *FASEB J* 2005;19:278–80.
  43. Levin MS, Talkad VD, Gordon JI, Stenson WF. Trafficking of exogenous fatty acids within Caco-2 cells. *J Lipid Res* 1992;33:9–19.
  44. Swinnen JV, Van Veldhoven PP, Esquet M, Heyns W, Verhoeven G. Androgens markedly stimulate the accumulation of neutral lipids in the human prostatic adenocarcinoma cell line LNCaP. *Endocrinology* 1996;137:4468–74.
  45. Ando H, Watabe H, Valencia JC, Yasumoto K, Furumura M, Funasaka Y, Oka M, Ichihashi M, Hearing VJ. Fatty acids regulate pigmentation via proteasomal degradation of tyrosinase: a new aspect of ubiquitin-proteasome function. *J Biol Chem* 2004;279:15427–33.
  46. McNeely W, Benfield P. Orlistat. *Drugs* 1998;56:241–9; discussion 50.
  47. Ho TS, Ho YP, Wong WY, Chi-Ming Chiu L, Wong YS, Eng-Choon Ooi V. Fatty acid synthase inhibitors cerulenin and C75 retard growth and induce caspase-dependent apoptosis in human melanoma A-375 cells. *Biomed Pharmacother* 2007;61:578–87.
  48. Chirala SS, Chang H, Matzuk M, Abu-Elheiga L, Mao J, Mahon K, Finegold M, Wakil SJ. Fatty acid synthesis is essential in embryonic development: fatty acid synthase null mutants and most of the heterozygotes die in utero. *Proc Natl Acad Sci USA* 2003;100:6358–63.
  49. Rossi S, Ou W, Tang D, Bhattacharya N, Dei Tos AP, Fletcher JA, Loda M. Gastrointestinal stromal tumours overexpress fatty acid synthase. *J Pathol* 2006;209:369–75.
  50. Ramaswamy S, Ross KN, Lander ES, Golub TR. A molecular signature of metastasis in primary solid tumors. *Nat Genet* 2003;33:49–54.
  51. Swinnen JV, Van Veldhoven PP, Timmermans L, De Schrijver E, Brusselmans K, Vanderhoydonc F, Van de Sande T, Heemers H, Heyns W, Verhoeven G. Fatty acid synthase drives the synthesis of phospholipids partitioning into detergent-resistant membrane microdomains. *Biochem Biophys Res Commun* 2003;302:898–903.
  52. Poste G, Doll J, Hart IR, Fidler IJ. In vitro selection of murine B16 melanoma variants with enhanced tissue-invasive properties. *Cancer Res* 1980;40:1636–44.
  53. Fidler IJ. Selection of successive tumour lines for metastasis. *Nat New Biol* 1973;242:148–9.
  54. Chan WS, Page CM, Maclellan JR, Turner GA. The growth and metastasis of four commonly used tumour lines implanted into eight different sites: evidence for site and tumour effects. *Clin Exp Metastasis* 1988;6:233–44.
  55. Kawada K, Sonoshita M, Sakashita H, Takabayashi A, Yamaoka Y, Manabe T, Inaba K, Minato N, Oshima M, Taketo MM. Pivotal role of CXCR3 in melanoma cell metastasis to lymph nodes. *Cancer Res* 2004;64:4010–17.
  56. Ito D, Back TC, Shakhov AN, Wiltrout RH, Nedospasov SA. Mice with a targeted mutation in lymphotoxin-alpha exhibit enhanced tumor growth and metastasis: impaired NK cell development and recruitment. *J Immunol* 1999;163:2809–15.
  57. Vantyghem SA, Postenka CO, Chambers AF. Estrous cycle influences organ-specific metastasis of B16F10 melanoma cells. *Cancer Res* 2003;63:4763–5.
  58. Browne CD, Hindmarsh EJ, Smith JW. Inhibition of endothelial cell proliferation and angiogenesis by orlistat, a fatty acid synthase inhibitor. *FASEB J* 2006;20:2027–35.